

## Supporting Information

### **Thermoregulatory elasticity braided fibers designed with core-sheath structure for wearable personal thermal management**

Chengcheng Wang,<sup>a</sup> Jingwen Wang,<sup>a</sup> Liping Zhang,<sup>\*a</sup> and Shaohai Fu<sup>a</sup>

<sup>a</sup> Jiangsu Engineering Research Center for Digital Textile Inkjet Printing, Key Laboratory of Eco-Textile, Jiangnan University, Ministry of Education, Wuxi, Jiangsu 214122, China.

\*E-mail: zhanglp@jiangnan.edu.cn

## Supplementary Methods

### 1. Characterization

The apparent morphology of the aerogel was characterized by a scanning electron microscopy (SEM, SU1510, Hitachi, Co., Ltd, Japan). The lamellar structure of MXene was observed by transmission electron microscope equipment (TEM, Hitachi JEM-2100). RT-IR spectra was measured by Nicolet 6700 spectrometer (Nicolet Instrument Company, Madison, WI, USA). The functional group was determined using a thermo ESCALAB 250Xi instrument equipped with a monochromatic Al K $\alpha$  (15 kV 5 mA) anode X-ray gun (XPS). The universal testing machine (UTM2203) equipped with a 100 N load cell was used to the compression test. The freezing-drying was carried out via the SCIENTZ-10 N freeze dryer (NingBo Scientz Biotechnology Co., Ltd, China). The color parameters of smart fabrics were obtained by computer color matching instrument (Datacolor DC850, America).

## Supplementary Figures

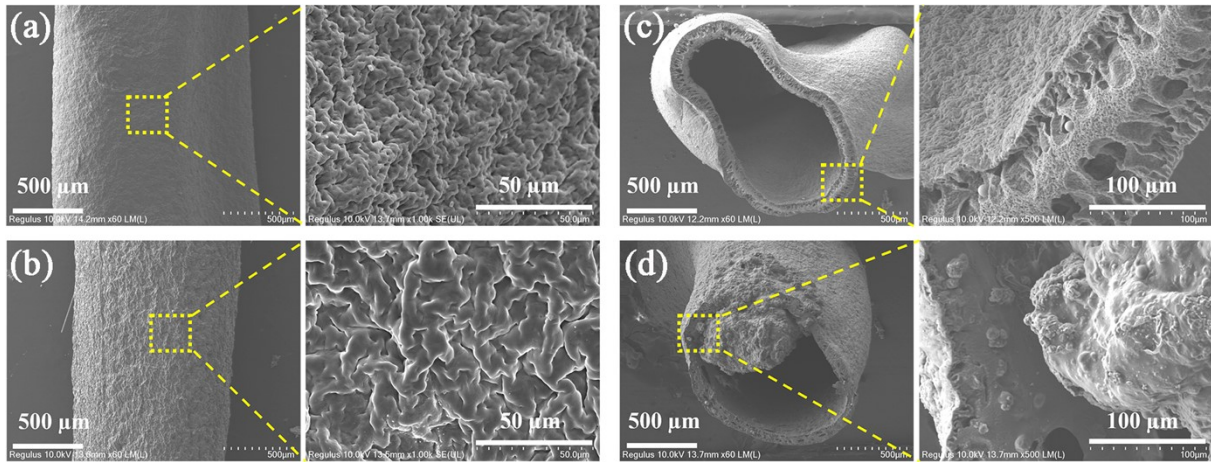


**Fig. S1** Surface morphologies and partial enlarged detail of (a) PU, and (b) PU@GA. Cross-section morphologies of (c) PU, and (d) PU@GA.

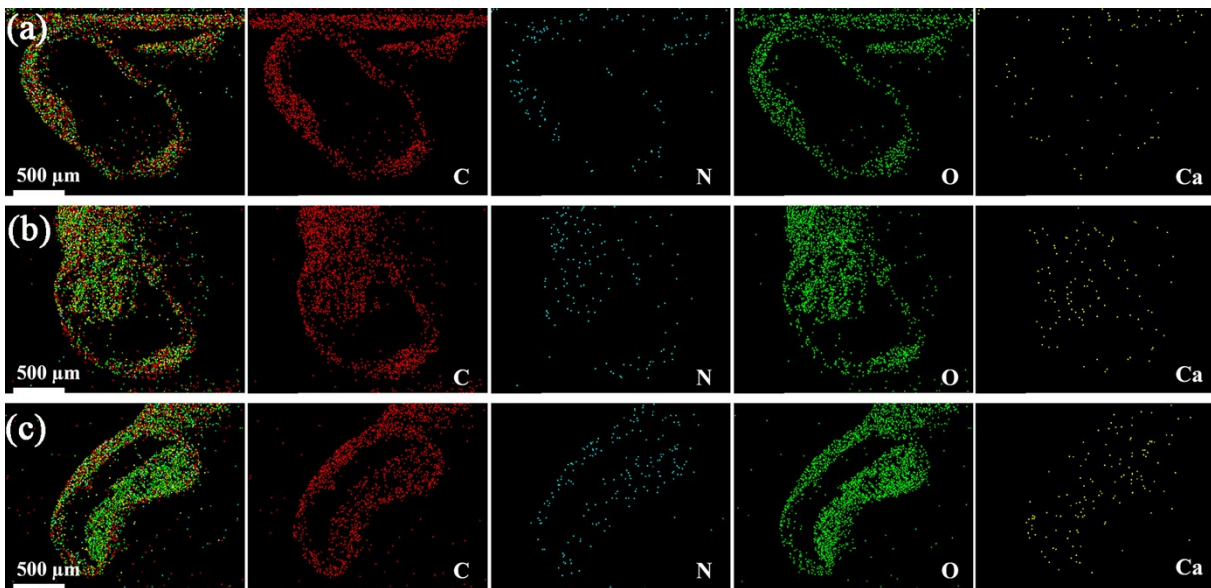


**Fig. S2** EDS-mapping images of (a) PU, (b) PU@GA, and (c) PU@GA@Ms.

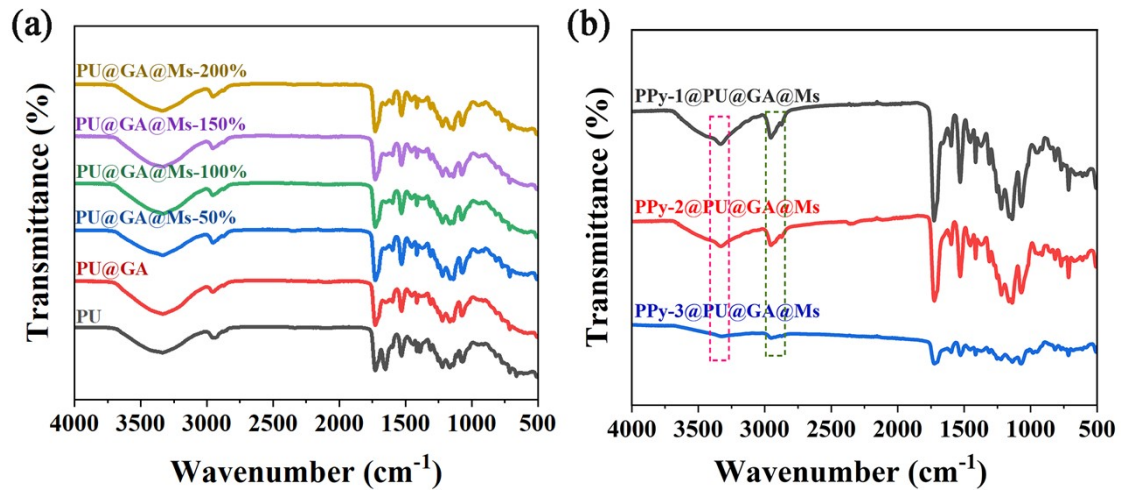


**Fig. S3** FTIR spectra of PU, PU@GA, PU@GA@Ms, and PPy@PU@GA@Ms.

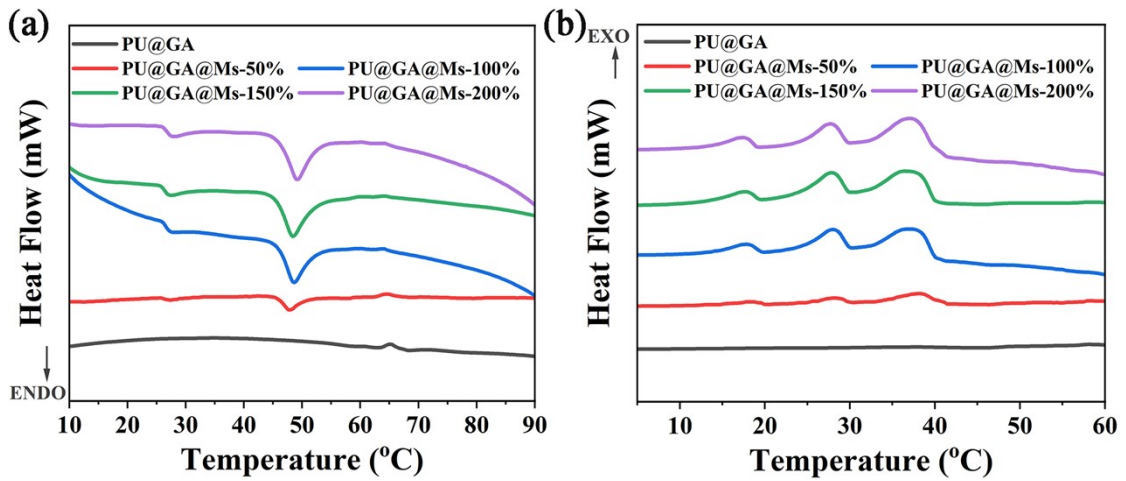


**Fig. S4** DSC curves of PU@GA and PU@GA@Ms-50%~200%.

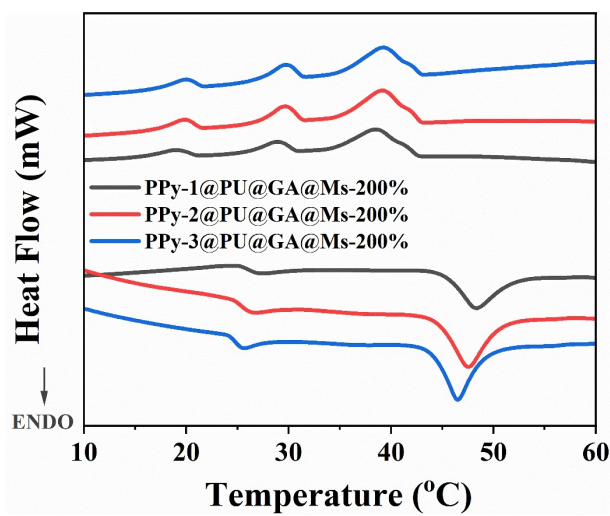


**Fig. S5** DSC curves of PPy@PU@GA@Ms in heating and cooling processes.

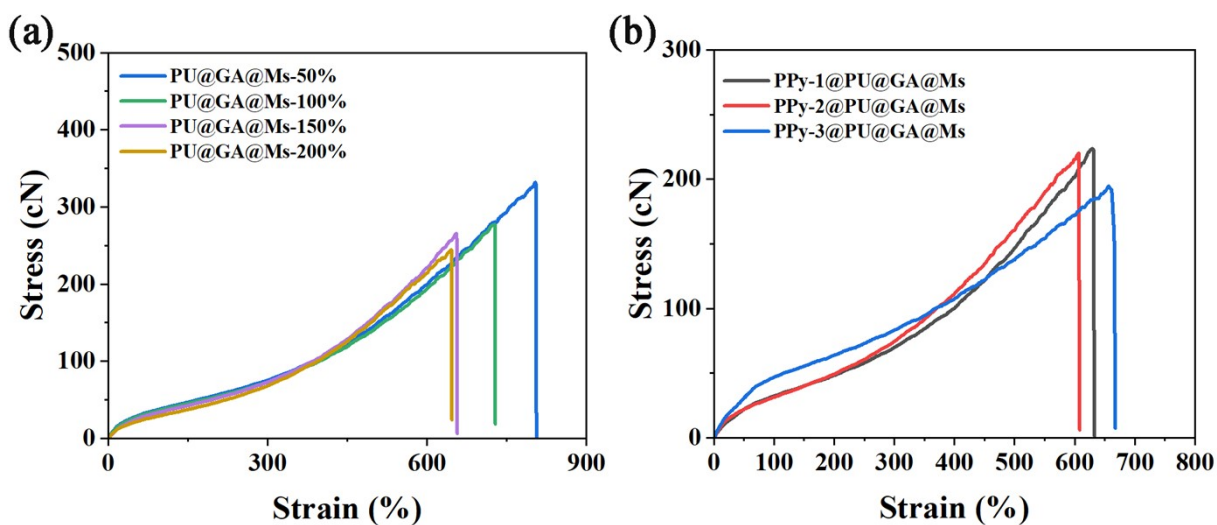


Fig. S6 Strain-stress curves of (a) PU@GA@Ms, and (b) PPy@PU@GA@Ms.

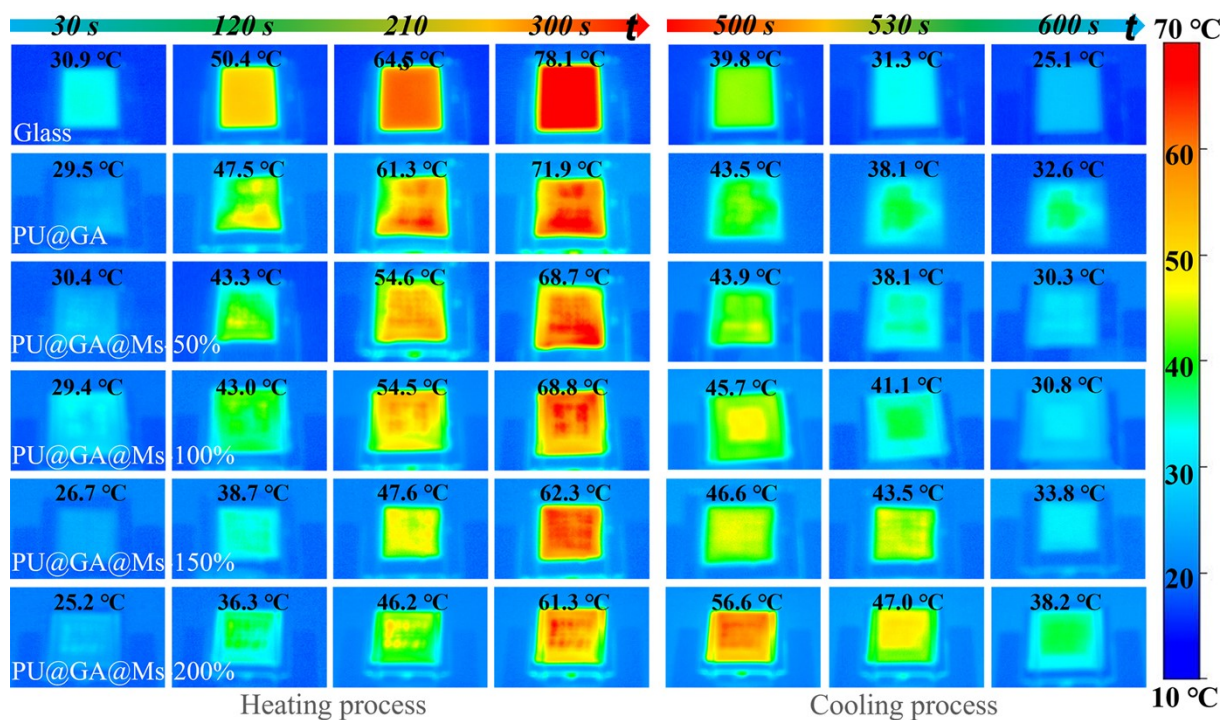
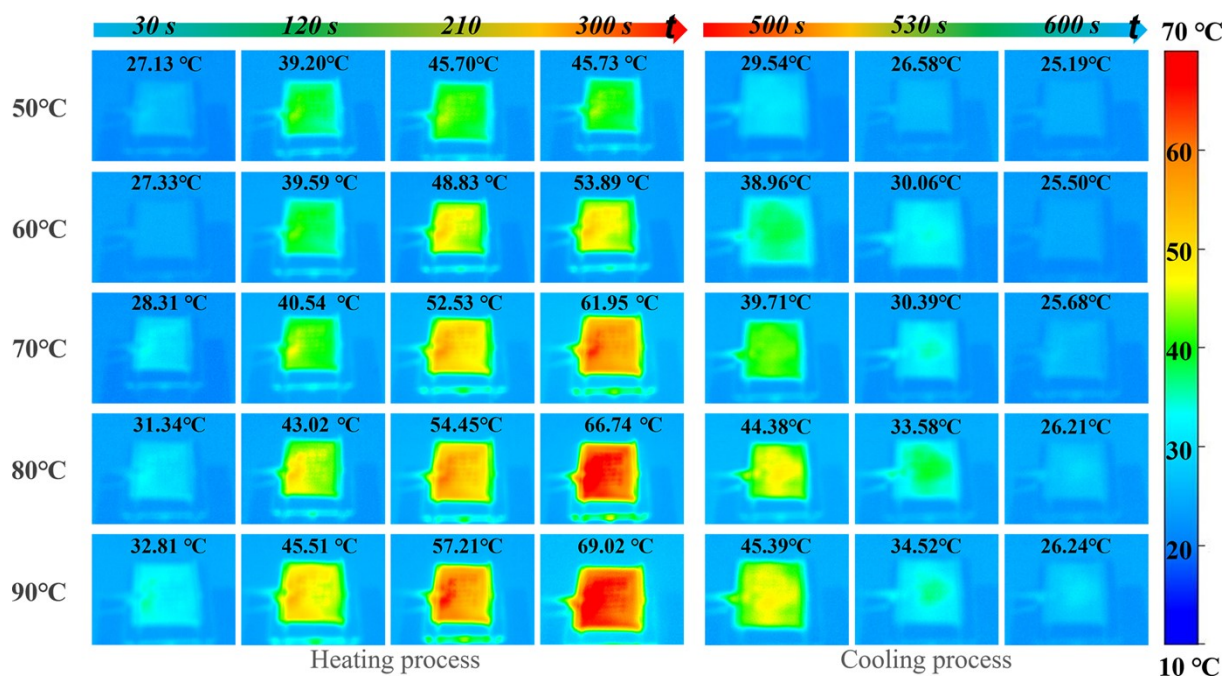
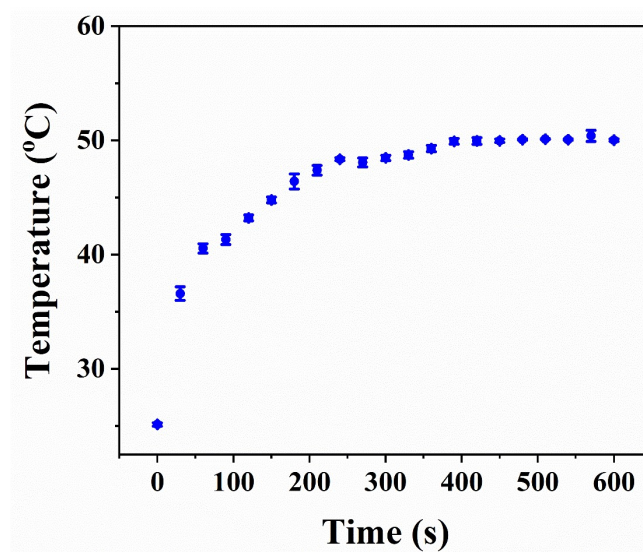


Fig. S7 IR thermal images of the pure glass sheet, PU@GA and PU@GA@Ms in the heating and cooling processes.



**Fig. S8** IR thermal images of PU@GA@Ms-200% at different initial heating temperature and natural cooling processes.



**Fig. S9** Surface temperature variation of PPy-3@PU@GA@Ms under  $1000 \text{ W}\cdot\text{m}^{-2}$  with different irradiation time.

## Supplementary Tables

Table S1 The thermal data and enthalpy of MPCM and fibers

Samples	$T_m$ (°C)	$T_c$ (°C)	$\Delta H_m$ (J/g)	$\Delta H_c$ (J/g)
PU@GA	--	--	0	0
MPCM	47.45	39.60	88.01	95.14
PU@GA@Ms-50%	47.78	38.23	31.07	31.18
PU@GA@Ms-100%	48.61	37.60	32.42	32.77
PU@GA@Ms-150%	48.39	37.35	33.28	33.23
PU@GA@Ms-200%	49.05	37.33	35.10	34.78
PPy-1@PU@GA@Ms-200%	47.74	38.65	34.67	35.06
PPy-2@PU@GA@Ms-200%	47.57	39.18	35.58	35.17
PPy-3@PU@GA@Ms-200%	46.01	39.18	37.15	36.60

Table S2 Electrical conductivity of the PPy@PU@GA@Ms fiber

	PPy-1@PU@GA@Ms (KΩ/cm)	PPy-2@PU@GA@Ms (KΩ/cm)	PPy-3@PU@GA@Ms (KΩ/cm)
1	19.4	11.3	10.4
2	17.4	12.5	9.6
3	18.8	10.8	10.2
Average value	18.5	11.5	10.1

Table S3 The comparison of photothermal conversion performance of fibers

Materials	Saturation Temperature (°C) 1000 W·m <sup>-2</sup>	Strain (%)	Morphology	Ref
PU/PPy/ZrC	55.8	150%	Coaxial wet spinning	S1
PW@PU@CNTs@PEDOT: PSS	70.5	264	Fibrous membrane	S2
PW@PDVB-12/PPy	47	--	--	S3
SF/CA	45	--	Silk Fiber	S4
AgNPs@PDA@PU@PW	63.2	--	Fibrous membrane	S5
PPy-PU/ZrC	78	291.57	Fibrous membrane	S6
PU/MXene@OD	65.3	--	Fiber	S7
PEG-PU-CNT	--	6	Composite membrane	S8
BPBBT CS-3	56.1	--	Fibrous membrane	S9
PPy@PU@GA@Ms	50.1	660	Fiber	This work

## Reference

- S1. Q. Yan, X. Du, Y. Liu, X. Zhou and B. Xin, *ACS Applied Materials & Interfaces*, 2022, **14**, 24820-24831.
- S2. J. Wu, M. Wang, L. Dong, J. Shi, M. Ohyama, Y. Kohsaka, C. Zhu and H. Morikawa, *ACS Nano*, 2022, **16**, 12801-12812.
- S3. L. Kong, Z. Wang, X. Kong, L. Wang, Z. Ji, X. Wang and X. Zhang, *ACS Applied Materials & Interfaces*, 2021, **13**, 29965-29974.
- S4. C. Wang, H. Dong, C. Cheng, K. Sun, T. Jin and Q. Shi, *ACS Sustainable Chemistry & Engineering*, 2022, **10**, 16368-16376.
- S5. J. Wu, M. Wang, L. Dong, Y. Zhang, J. Shi, M. Ohyama, Y. Kohsaka, C. Zhu and H. Morikawa, *Chemical Engineering Journal*, 2023, **465**, 142835.
- S6. Q. Yan, B. Xin, Z. Chen and Y. Liu, *Materials Today Communications*, 2021, **28**, 102584.
- S7. J. Zhang, Y. Zhang, S. Wu, Y. Ji, Z. Mao, D. Wang, Z. Xu, Q. Wei and Q. Feng, *Chemical Engineering Journal*, 2024, **483**, 149281.
- S8. J. Shi, W. Aftab, Z. Liang, K. Yuan, M. Maqbool, H. Jiang, F. Xiong, M. Qin, S. Gao and R. Zou, *Journal of Materials Chemistry A*, 2020, **8**, 20133-20140.
- S9. H. Li, H. Wen, Z. Zhang, N. Song, R. T. K. Kwok, J. W. Y. Lam, L. Wang, D. Wang and B. Z. Tang, *Angewandte Chemie International Edition*, 2020, **59**, 20371-20375.